Multiparametric functional MRI of the kidneys – evaluation of test-retest repeatability and effects of different manual and automatic image analysis strategies

Multiparametrische funktionelle MRT der Nieren – Evaluation der Wiederholbarkeit und des Effektes verschiedener manueller und automatischer Bildanalysestrategien

Authors

Cecilia Liang[1], Isabelle Loster[2], Stephan Ursprung[1], Aya Ghoul[3], Thomas Küstner[3], Brigitte Gückel[1], Bernd Kühn[4], Fritz Schick[5], Petros Martirosian[5], Ferdinand Seith[1]

Affiliations

1 Department of Diagnostic and Interventional Radiology, University Hospital Tübingen, Tübingen, Germany
2 Faculty of Medicine, Eberhard Karls University Tübingen, Tübingen, Germany
3 Medical Image and Data Analysis (MIDAS.lab), Department of Diagnostic and Interventional Radiology, University Hospital Tübingen, Tübingen, Germany
4 Siemens Healthcare AG, Erlangen, Germany
5 Section on Experimental Radiology, Departement of Diagnostic and Interventional Radiology, University Hospital Tübingen, Tübingen, Germany

Keywords

MRI, segmentation, kidney

received 17.8.2024
accepted after revision 10.11.2024
published online 2025

Bibliography

Fortschr Röntgenstr
DOI 10.1055/a-2480-4885
ISSN 1438-9029

Georg Thieme Verlag KG, Oswald-Hesse-Straße 50, 70469 Stuttgart, Germany

Correspondence

Cecilia Liang
Department of Diagnostic and Interventional Radiology, University Hospital Tübingen, Tübingen, Germany
cecilia.liang@med.uni-tuebingen.de

ABSTRACT

Objective Multiparametric MRI is a promising technique for noninvasive structural and functional imaging of the kidneys that is gaining increasing importance in clinical research. Still, there are no standardized recommendations for analyzing the acquired images and there is a need to further evaluate the accuracy and repeatability of currently recommended MRI parameters. The aim of the study was to evaluate the test-retest repeatability of functional renal MRI parameters using different image analysis strategies.

Methods Ten healthy volunteers were examined twice with a multiparametric renal MRI protocol including arterial spin labeling (ASL), diffusion-weighted imaging (DWI) with intravoxel incoherent motion (IVIM), blood-oxygen-dependent (BOLD) imaging, T1 and T2 mapping, and volumetry with an interval of one week. The quantitative results of both kidneys were determined by manual organ segmentation, ROI analysis, and automatic segmentation based on the nnUNet framework. Test-retest repeatability of each parameter was computed using the within-subject coefficient of variance (wCV) and the intraclass coefficient (ICC). Segmentation accuracy and inter-reader agreement were evaluated using the dice score.

Results Structural tissue parameters (T1, T2) showed wCV (%) between 4 and 11 and an ICC between 0.2 and 0.8. Functional parameters (ASL, BOLD and DWI) showed wCV (%) between 3 and 38 and an ICC between 0.0 and 0.7. The highest variances between test-retest scans were observed in perfusion measurements with ASL and IVIM (wCV: 17–37 %). Quantitative analysis of the cortex and medulla showed a better repeatability when acquired using manual segmentation compared to ROI-based image analysis. Comparable repeatability was achieved with manual and automatic segmentation of the total kidney.

Conclusion Reasonable repeatability was achieved for all MR parameters. Structural MR parameters showed better repeatability compared to functional parameters. ROI-based image analysis showed overall lower repeatability compared to manual segmentation. Comparable repeatability to manual segmentation as well as acceptable segmentation accuracy could be achieved with automatic segmentation.

Key Points

- Reasonable test-retest repeatability can be achieved with multiparametric MRI of the kidneys.
- Image analysis based on manual segmentation of the cortex and medulla showed overall better repeatability compared to ROI-based analysis.

- Automatic segmentation of kidney volume showed similar repeatability of quantitative image analysis compared to manual segmentation.

Citation Format

- Liang C, Loster I, Ursprung S et al. Multiparametric functional MRI of the kidneys - evaluation of test-retest repeatability and effects of different manual and automatic image analysis strategies. Fortschr Röntgenstr 2025; DOI 10.1055/a-2480-4885

ZUSAMMENFASSUNG

Einleitung Die multiparametrische MRT ist eine vielversprechende Technik zur nicht-invasiven strukturellen und funktionellen Bildgebung der Nieren, welche an zunehmender Bedeutung in der klinischen Forschung gewinnt. Allerdings gibt es noch keine standardisierten Empfehlungen zur Auswertung der erhobenen Bilddaten und auch die derzeit empfohlenen MR-Parameter müssen weiter hinsichtlich ihrer Genauigkeit und Wiederholbarkeit untersucht werden. Ziel dieser Studie war die Evaluation der Test-Retest-Wiederholbarkeit der funktionellen MR-Parameter an der Niere unter Verwendung verschiedener Strategien zur Bildanalyse.

Material und Methoden 10 gesunde Probanden wurden zweimal mit Abstand einer Woche mittels eines multiparametrischen MR-Protokolls der Nieren untersucht, welches folgende Parameter umfasste: arterial spin labeling (ASL), diffusion-weighted imaging (DWI) with intravoxel incoherent motion (IVIM), blood-oxygen-dependent (BOLD) imaging, T1 und T2 mapping und die Volumetrie. Die quantitativen Ergebnisse beider Nieren wurden mittels manueller Segmentierung, ROI-Analyse und automatischer Segmentierung basierend auf dem nnUNet framework erhoben. Die Test-Retest Wiederholbarkeit der einzelnen Parameter wurde mittels within-subject Variationskoeffizienten (wCV) und des Intraklassen-Korrelationskoeffizienten (ICC) ermittelt. Die Segmentierungsgenauigkeit sowie die Übereinstimmung zwischen den Bewertern wurde mittels Dice score evaluiert.

Ergebnisse Strukturelle Gewebeparameter (T1, T2), zeigten eine wCV zwischen 4 und 11 % sowie einen ICC zwischen 0,2 und 0,8. Funktionelle Parameter (ASL, BOLD und DWI) wiesen einen wCV zwischen 3 und 38 auf sowie einen ICC zwischen 0,0 und 0,7. Die höchste Varianz zwischen den Test-Retest-Scans konnte bei den Perfusionsmessungen (ASL und IVIM) beobachtet werden mit einem wCV zwischen 17 bis 37 %. Die quantitative Analyse des Nierenkortex sowie der Medulla zeigte insgesamt eine bessere Wiederholbarkeit unter Verwendung der manuellen Segmentierung im Vergleich zur ROI-Analyse. Eine vergleichbare Wiederholbarkeit zur manuellen Segmentierung konnte mit der automatischen Segmentierung erzielt werden.

Schlussfolgerung Insgesamt zeigten alle angewandten MR-Parameter eine akzeptable Test-Retest-Wiederholbarkeit. Strukturelle MR-Parameter zeigten eine bessere Wiederholbarkeit im Vergleich zu funktionellen Parametern. Mittels ROI-Analyse erhobene Daten wiesen eine geringere Wiederholbarkeit im Vergleich zu mittels manueller Segmentierung erhobenen Daten auf. Eine mit der manuellen Segmentierung vergleichbare Wiederholbarkeit sowie eine akzeptable Segmentierungsgenauigkeit konnte mittels automatischer Segmentierung erzielt werden.

Kernaussagen

- Eine angemessene Test-Retest-Wiederholbarkeit kann mittels multiparametrischer MRT der Nieren erreicht werden.
- Die manuelle Segmentierung des Kortex und der Medulla zeigte insgesamt eine bessere Wiederholbarkeit im Vergleich zur der ROI-Analyse.
- Die automatische Segmentierung des Nierenvolumens zeigte eine mit der manuellen Segmentierung vergleichbare Wiederholbarkeit bzgl. der quantitativen Bildanalyse.

Abbreviations

AKI	Acute kidney injury
ASL	Arterial spin labeling
BOLD	Blood-oxygenation-level-dependent
CKD	Chronic kidney disease
COST	Cooperation of Science and Technology
D	Diffusion coefficient
DWI	Diffusion weighted imaging
EPI	Echo-planar imaging
FLASH	Fast low angle shot
FOCI	Frequency offset corrected inversion
F	Perfusion fraction
ICC	Intraclass correlation coefficient
IVIM	Intravoxel incoherent motion
mGRE	Multi-echo spoiled gradient echo
MOLLI	Modified look-locker inversion recovery
MRI	Magnetic resonance imaging
PCASL	Pseudo-continuous arterial spin labeling
RBF	Renal blood flow
RC	Repeatability coefficient
ROI	Region of interest
TE	Echo time
TR	Repetition time
VFA	Variable Flip angle
wCV	Within-subject coefficient of variations
wSD	Within-subject standard deviation

Introduction

Multiparametric quantitative magnetic resonance imaging (MRI) is gaining attention in research but still needs to prove its role in clinical kidney diagnostics. As a noninvasive modality without radiation exposure and no need for potentially nephrotoxic contrast

▶ **Table 1** Overview of functional MRI techniques for renal imaging

MRI technique	MRI measure	Biomarker	Application
Arterial Spin Labeling (ASL)	Renal blood flow (ml/100 mL/min)	Tissue perfusion	Renal artery stenosis Kidney transplant dysfunction Acute kidney injury Chronic kidney diseases Renal masses
Diffusion-weighted imaging (DWI)	Diffusion (mm^2/sec)	Tissue diffusion; changes in microstructure due to fibrosis, cellular infiltration, or edema	Kidney transplant dysfunction Acute kidney injury Chronic kidney diseases Renal masses Inflammatory diseases
Blood oxygen-dependent (BOLD) MRI	T2* map (ms)	Tissue oxygenation; changes in the microstructure of the capillary bed	Renal artery stenosis Kidney transplant dysfunction Acute kidney injury
T1 & T2 mapping	T1/T2 relaxation time (ms)	Tissue characterization, changes in molecular environment (water content, fibrosis, inflammation)	Kidney transplant dysfunction Chronic kidney diseases

agents, MRI is especially attractive for renal imaging. A broad range of MRI techniques has been reported to be useful for the assessment of structural and functional information of the kidneys. Renal perfusion, which is a critical element in the development of various kidney diseases, such as acute kidney injury (AKI) and chronic kidney disease (CKD), can be quantified using arterial spin labeling (ASL) techniques [1]. Diffusion-weighted imaging (DWI) can help to detect pathologies in microstructure caused by fibrosis for instance [2]. Tissue oxygenation also plays an important role in renal pathophysiology and can be depicted by blood oxygenation level-dependent (BOLD) imaging [3]. Other MRI parameters such as T1 and T2 can provide deeper insight into structural changes in kidney tissue [4]. An overview of the most common MRI techniques for functional imaging of the kidneys is provided in ▶ **Table 1**.

Although all these parameters seem to play an important role in different pathologies of the kidneys, it should be noted that they can only be determined by MRI and there is no noninvasive gold standard for comparison with the acquired results. For clinical studies with different patient groups or longitudinal clinical trials, it is, therefore, even more important to understand the measurement-related variance of the resulting data. Derived values might also depend on the method used for image analysis.

In the past decades, several research groups have applied multiparametric MRI protocols to examine kidneys in healthy volunteers and patients with different kidney diseases [5, 6, 7, 8, 9, 10, 11, 12, 13, 14, 15, 16, 17, 18, 19, 20]. Even though repeatability studies have been performed for different MRI parameters, the diversity of MRI protocols, post-processing, and analysis strategies hinders the comparability of these studies and thus impedes the final assessment of clinical applicability [21, 22].

In view of these difficulties, joint recommendations concerning renal MRI protocols have been developed by a pan-European network of researchers in renal MRI (PARENCHIMA) funded by the European Cooperation of Science and Technology (COST) to harmonize and standardize data collection approaches [23]. These recommendations comprise proposals for the composition of MRI protocols, settings, and readout techniques, but they also point out missing evidence for the best settings and applications [22, 24, 25, 26, 27].

Considering the rising amount of medical imaging, fast image analysis techniques are gaining importance [28]. Automatic segmentation approaches using deep learning are sought, but as they are still in progress and lack broader availability, manual segmentation remains an essential analysis technique also used for training data when developing automatic segmentation tools. To our knowledge, however, there is no study evaluating different manual segmentation techniques and automatic segmentation for the kidney concerning reproducibility.

Further studies on repeatability, reliability, and validity of multiparametric functional MRI protocols and analysis strategies for kidney diagnostics pave the way for larger clinical trials and finally transfer to the clinical setting.

The aim of this study was to evaluate a multiparametric renal functional MRI protocol, guided by the PARENCHIMA recommendations, on the test-retest reliability using two different established manual image analysis techniques including manual tissue segmentation and representative region of interest (ROI)-based analysis as well as deep learning-based automatic segmentation.

Methods

This study is the first subgroup analysis of a prospectively conducted study. The study was approved by the local ethics committee and all volunteers gave written informed consent regarding the examination and the scientific evaluation of their data.

▶ **Table 2** Overview of the multiparametric MRI protocol. (Resp. comp.: respiratory compensation; FB: free breathing; NAV: navigated breathing; BH: breath-hold; MBH: multiple breath-holds; BW: readout bandwidth; TF: Turbo FLASH).

	ASL	DWI	BOLD	T1 mapping	T2 mapping	Volumetry
Sequence	PCASL	IVIM	mGRE	VFA	T2prep TFL	VIBE
TR (ms)	6000–7400	1500	133	3.5	5000	3.95
TE (ms)	27.46	55.0	2.46–46.74	1.24	2.59	1.23/2.46
Flip angle (deg)	90/180	90/180	40	2, 10	8	8
BW (Hz/Px)	3064	2004	400	430	490	890
Matrix	96×48×24	192×96×24	256×205×12	256×205×32	256×205	256×205×32
FOV (mm^3)	380×380×144	380×380×72	380×380×54	380×380×96	380×380×8	380×380×96
Voxel size (mm^3)	4.0×4.0×6.0	1.5×1.5×3.0	1.5×1.5×3.0	1.5×1.5×3.0	1.5×1.5×8.0	1.5×1.5×3.0
Resp. comp.	FB	NAV	MBH	BH	NAV	BH
Scan time (min)	4:18	5–10	3:30	0:15	3–4	0:16

Subjects

Ten healthy volunteers were examined twice with one week between visits. The same time of day and identical scanning protocols were selected for both examinations to be compared. Exclusion criteria were a history of renal or cardiovascular disease, contradictions for MRI, and implants near the kidney region. Volunteers were asked to avoid salt and protein-rich meals and above-average amounts of coffee on the day of examination as well as liquids and larger meals 2 hours before the MRI scan but were instructed to drink regular amount of liquids throughout the day.

Imaging protocol

Images were acquired using a 3 T whole-body MRI system (MAGNETOM Prisma^{fit}, Siemens Healthcare, Erlangen, Germany) with an 18-channel matrix-array coil in combination with 12 channels of a spine-array coil. The examination protocol included several sequences for functional imaging:

a) A 3 D single-shot pseudo-continuous ASL (PCASL) research sequence with optimized turbo gradient spin echo (TGSE) readout for contrast-free perfusion imaging [29]. The four non-selective hyperbolic secant inversion pulses in combination with the selective pre-saturation and frequency offset corrected inversion (FOCI) pulses ensure efficient saturation of the background signal. 10 pairs of images with labeling duration of 1500 ms, post-labeling duration of 1500 ms, and labeling flip angle of 25°. The ten label-control image pairs and an M0 scan were acquired under free breathing.

b) A diffusion-weighted single-shot echo-planar imaging (EPI) research sequence with reduced field of view (zoomed) for intravoxel incoherent motion (IVIM) imaging; a four-directional diffusion mode 4-scan trace with monopolar diffusion gradient scheme and b-values of 0, 10, 30, 50, 70, 100, 150, 200, 400, and 800 s/mm^2 was applied. Two sets of DWI data were acquired with the phase-encoding direction reversed (head to feet and feet to head) to enable the geometric distortion correction resulting from EPI acquisition [30].

c) A multiple-echo spoiled gradient echo (mGRE) sequence for BOLD imaging. Ten echoes with $TE_1 = 2.46$ ms and $\Delta TE = 4.92$ ms were acquired. Images were acquired with navigator triggering under free breathing.

d) A 3 D variable flip angle (VFA) approach using a volumetric interpolated breath-hold examination (VIBE) sequence as well as a 2 D inversion recovery technique using a modified look-locker inversion recovery (MOLLI) sequence for T1 mapping.

e) A 2 D T2prep turbo fast low angle shot (FLASH) sequence for T2 mapping. The measurement consisted of 24 repetitions with a continuously increasing echo time of the preparation module: $TE_1 = 8$ ms and $\Delta TE = 8$ ms. At the start, a measurement without preparation was performed.

Additionally, 2 D T1-weighted GRE and T2-weigthed half-Fourier acquisition single-shot turbo spin echo (HASTE) anatomical images were acquired and 3 D T1-weighted volumetric interpolated breath-hold examination (VIBE) imaging was performed for volumetric analysis. Details of the imaging protocol are summarized in ▶ **Table 2**. Anatomical images, T1 mapping, and BOLD images were acquired during breath-hold. IVIM measurements as well as T2 mapping were performed using navigator gating. ASL data were measured under free breathing conditions. The total scan time was approximately 45 minutes.

Post-processing of MRI data

a) For ASL data, motion correction was performed retrospectively using 3 D elastic registration software (provided by the manufacturer). Renal blood flow (RBF) maps were then calculated based on the Buxton model [31] using the expression given in Eq. 1 by Robson et al. [32]. A constant T1 of 1200 ms was assumed for the entire kidney and a T1 of 1600 ms was used for blood. Other parameters were: arrival time: 750 ms; labeling duration: 1500 ms; post-labeling delay: 1500 ms; inversion

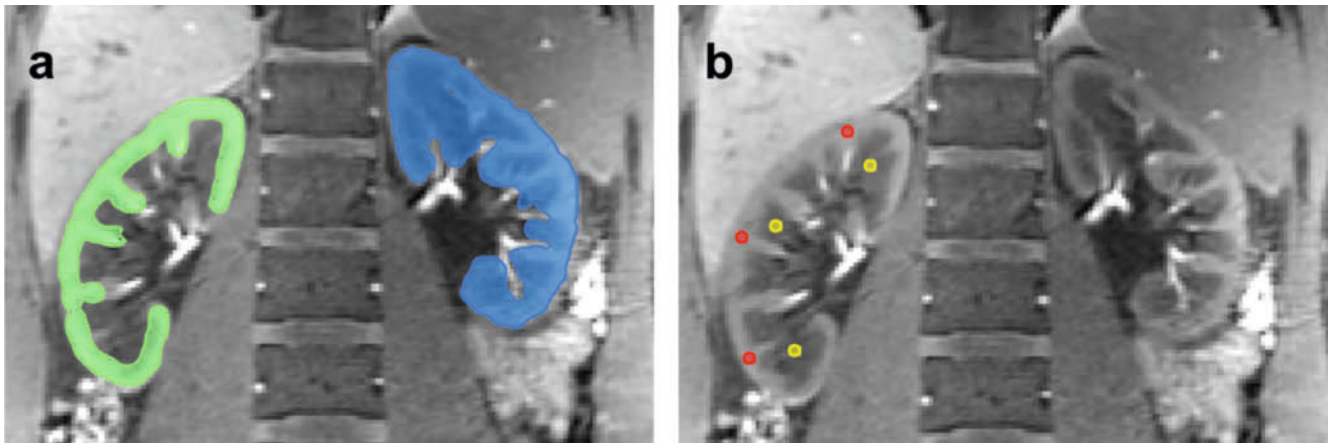

▶ **Fig. 1** Example of masks created on anatomical T1-weighted images by **a** manual segmentation of the cortex (right kidney, green) and the total kidney (left kidney, blue) and by **b** placement of ROIs on the cortex (red circles) and medulla (yellow circles).

efficiency: 0.8; additional inversion inefficiency from background suppression pulses: 0.75; tissue/blood partition coefficient: 0.9 ml/g.

b) For diffusion data, image processing was applied by using the FMRIB-FSL (v. 6.0.7) library for the left and right kidneys separately [33]. In particular, the susceptibility-induced geometric distortions were corrected by FSL *topup* using the additional DWI data with reversed phase-encoding direction. Moreover, eddy-current distortions, volume-to-volume movement, and slice-to-volume movement were corrected with FSL *eddy* [34]. Diffusion coefficient (D) maps and perfusion fraction (f) maps were calculated based on the IVIM model [35]. To obtain more stabilized IVIM parameters, we used a 2-step fitting procedure (also known as segmented fitting) in which D was estimated using higher b-values (b = 200, 400, 800). Once D was estimated, an additional data point, $S_{intercept}$, at b = 0 was introduced to allow calculation of the perfusion fraction using the equation: $f = (S_0 - S_{intercept})/S_0$), where S_0 is the measured signal by b = 0 [36].
c) For BOLD data, no motion correction was required. T2* maps were calculated using manufacturer software on the scanner.
d) For T1 mapping using the VFA approach, B1 + inhomogeneities were corrected using B1-mapping scan from the manufacturer. In addition, respiratory movements were corrected using FSL *flirt* image registration [33]. Finally, T1 maps were calculated by linear regression.
e) For T2 mapping, motion correction was performed before quantitative evaluation using LAP image registration [37]. Data was fitted to a monoexponential model in a voxel-wise manner.

Image analysis

Manual image segmentation

Manual image analysis was performed on a standalone PC by a radiologist with 6 years of experience in functional MR imaging analysis of the kidneys. For evaluation of inter-reader agreement, 2 additional readers with several years of experience in renal research segmented anatomical T1 images.

Two different techniques were applied to manually define the renal components for the subsequent extraction of functional information. On the one hand, representative ROIs were located on the cortex and medulla on a central image slice. For each structure, 3 circular ROIs were placed on the superior pole, middle part, and inferior pole on a single central image slice. On the other hand, the renal cortex and the total kidney excluding the renal pelvis were segmented manually on all image slices. The medullary components were calculated from the total kidney and cortex segmentation masks. Both ROI image analysis and manual segmentation were performed on the NORA Medical Imaging Platform (University Medical Center Freiburg [38]). ROI and segmentation masks were extracted in the next step for functional analysis. ▶ **Fig. 1** gives an example of the masks created on NORA by manual segmentation and placement of ROIs.

Automatic segmentation

We based the configuration of the segmentation model on the nnU-Net framework [39]. A 5-level 2D U-Net architecture was chosen that operates using deep supervision. The outputs of the three highest resolutions in the decoder were used to form the final segmentation mask. The input patch size was selected to be 192 × 128. The first encoding level had 32 convolutional kernels that are doubled after each downsampling with a maximum of 320 kernels at the bottleneck. The decoder's kernel count reflected that of the encoder. Leaky ReLU with slope of 0.01 and batch normalization were applied after every convolution.

We ran a four-fold cross-validation. The training loss consisted of the sum of the Dice score and cross-entropy loss and operated on 2 class labels including the left and right kidneys, calculated at the full resolution output and the auxiliary outputs of lower resolution. Different data augmentation strategies were applied on the fly during training to help the model learn transformation invariant features including rotation, cropping, scaling, additive brightness and contrast to the input images, and elastic transformations. Training was conducted with stochastic gradient descent with an initial learning rate of 0.01, decaying with a polynomial schedule [40], and a Nesterov momentum of 0.99 and ran for a

total of 1000 epochs with a batch size of 8, where one epoch is defined as 500 iterations. The Dice score on the current validation set was used to monitor the training progress.

Statistical analysis

Mean values were obtained from the 3 ROIs placed on the cortex and medulla of each kidney. To assess agreement of test-retest measurements, the repeatability coefficient (RC) and the within-subject coefficients of variations (wCV) were calculated based on the within-subject standard deviation (wSD) as:

$$RC = 2.77 \times wSD \text{ and } wCV = 100 \times \frac{wSD}{m}$$

and

$$wSD = \sqrt{\frac{1}{2n}\sum_{i}^{n} d_i^2}$$

where d and m are the difference and mean values for scan-rescan measurements and n is the number of subjects. Additionally, the intra-class correlation coefficient (ICC) was calculated, and Bland-Altman plots were used to evaluate the agreement between test-retest scans with limits of agreement calculated as the mean difference ± 1.96 SD of difference. Scatterplots were generated to visualize agreement between test-retest scans comparing different renal compartments and image analysis. A paired t-test was used to analyze the difference between segmentation strategies, kidney sides, and renal compartments with $p < 0.05$ considered statistically significant. Moreover, we also analyzed the repeatability of the ratio of each parameter of the right and left kidney. The Dice score was used to determine the inter-reader agreement between the 3 readers for manual tissue segmentation of anatomical T1 images and the accuracy of automatic segmentation.

Analyses were carried out using MATLAB (The MathWorks, Natick, MA) and SPSS (IBM Corp., IBM SPSS Statistics, Version 27.0, Armonk, NY) software.

Results

Ten healthy volunteers (age range between 19 and 41, 5 female participants) were successfully examined. ▶ **Table 3** provides an overview of all calculated repeatability measures. ▶ **Fig. 2** depicts kidney images of a healthy volunteer examined with the multiparametric MRI protocol.

Segmentation

Manual segmentation of the total kidney volume was performed for all MR parameters. Manual segmentation of the cortex could be performed for ASL, BOLD, and T1 maps. Medulla masks could be obtained by subtraction for T2* and T1 maps. Automatic segmentation of the kidney volume was performed for ASL, DWI, BOLD, and VIBE. ROI analysis for the cortex and medulla was performed for all parameters.

Test-retest repeatability

Test-retest repeatability of functional MRI measurements varied depending on MR parameters, kidney compartment, kidney side, and image analysis strategy.

Comparing different functional MR parameters, best repeatability could be achieved with DWI (wCV 2.85–5.13 %), followed by BOLD (wCV 3.69–10.18 %), T1 map (wCV 4.01–11.05 %), and T1 map (wCV 5.93–7.95 %), whereas perfusion measurement with ASL and the perfusion fraction derived from IVIM resulted in considerably lower repeatability (RBF: wCV 17.96–20.28 %, f: wCV 17.02–7.39 %). The repeatability of volume measurements with manual and automated segmentation was moderate with wCV between 6.51 % and 10.51 % and relatively low for cortex volume by manual segmentation.

In the comparison of kidney compartments, there was no significant difference in repeatability of MR values of different parameters between the medulla and cortex except for perfusion measurements with ASL and the perfusion fraction derived from IVIM ($p < 0.05$).

Comparing different image analysis strategies, ROI analysis of the cortex and medulla showed significantly less repeatability ($p < 0.05$) compared to manual segmentation of the cortex and medulla in T1 and T2* maps. ROI analysis in RBF maps achieved similar repeatability results to manual segmentation. There were no significant differences in quantitative values between automatic segmentation and manual segmentation of the total kidney across all parameters. Repeatability was slightly better for manual segmentation in almost all parameters and in volumetry except for the perfusion fraction (f) derived from IVIM.

There was no significant difference concerning quantitative measurements and repeatability between the right and left kidney across all parameters. There was also no significant difference in repeatability between the cortex and medulla except for perfusion measurements with ASL and IVIM ($p < 0.05$).

Inter-reader agreement

The inter-reader agreement across all 3 readers for manual segmentation of anatomical T1 images was acceptable for segmentation of the total kidney with Dice scores between 0.79 and 0.86, but considerably lower for segmentation of the cortex with an average dice score between 0.66 and 0.76.

Accuracy of automatic segmentation

Automatic segmentation was applied for VIBE, ASL, DWI, and BOLD. Manual segmentation served as the ground truth reference. Automatic segmentation using the nnU-net framework showed overall acceptable accuracy with Dice scores between 0.86 and 0.92 displayed in ▶ **Fig. 3**. The highest segmentation accuracy was achieved with anatomical VIBE and diffusion maps (0.91), while segmentation of RBF images showed the lowest segmentation accuracy (0.86). ▶ **Fig. 4** shows examples of automatic segmentation masks (lower row, red) compared to manually segmented masks (upper row, green).

▶ **Table 3** Overview of the test-retest repeatability evaluation of the multiparametric functional MRI protocol. MOS: manual organ segmentation; AOS: automatic organ segmentation; ROI: region of interest; SD: standard deviation; RC: repeatability coefficient; wCV: within subject coefficient of variation; ICC: intraclass correlation coefficient; D: diffusion coefficient; f: perfusion fraction.

				Baseline		Follow-up		Bias (%)	RC	WCV (%)	ICC
Parameter	**Unit**	**Segmentation**		**Mean**	**SD**	**Mean**	**SD**				
RBF	mL/100 mL/min	MOS	Total kidney	190.12	33.50	179.38	36.25	5.25	91.92	17.96	0.14
			Cortex	224.67	48.06	216.80	38.77	−1.00	122.09	19.97	0.00
		AOS	Total kidney	230.59	50.35	208.02	39.58	11.85	109.64	18.05	0.33
		ROI	Cortex	167.41	40.18	140.45	36.81	23.60	86.46	20.28	0.49
			Medulla	199.45	33.79	180.63	33.66	12.40	89.20	16.95	0.22
D	$10^{-6}mm^2/s$	MOS	Total kidney	1565.94	60.74	1558.67	62.22	0.38	123.53	2.85	0.49
		AOS	Total kidney	1563.94	56.96	1563.56	61.60	−0.05	128.17	2.96	0.40
		ROI	Cortex	1575.21	108.32	1598.54	109.34	−1.81	242.27	5.51	0.38
			Medulla	1490.91	81.33	1515.42	93.92	−1.86	213.57	5.13	0.27
f	%	MOS	Total kidney	17.94	3.52	17.94	3.69	−2.32	8.46	17.02	0.29
		AOS	Total kidney	17.83	3.39	18.07	3.39	−3.51	7.67	15.43	0.34
		ROI	Cortex	19.41	4.89	18.58	5.95	1.68	12.16	23.12	0.37
			Medulla	18.20	6.72	16.17	6.59	−10.22	17.80	37.39	0.11
T2*map	ms	MOS	Total kidney	51.05	3.07	51.43	3.91	−0.77	5.24	3.69	0.72
			Cortex	56.41	3.79	56.05	4.26	0.52	6.16	3.96	0.71
			Medulla	44.50	3.23	45.20	4.92	−1.74	9.45	7.61	0.35
		AOS	Total kidney	51.00	2.91	51.29	4.18	−0.58	5.97	4.22	0.65
		ROI	Cortex	57.22	7.11	56.27	9.85	0.58	20.96	13.33	0.24
			Medulla	43.62	8.10	44.56	7.70	−4.62	12.43	10.18	0.69
T1 map	ms	MOS	Total kidney	1672.63	101.53	1697.44	60.51	−1.78	187.07	4.01	0.39
			Cortex	1543.71	101.54	1569.04	64.45	−1.92	162.11	3.76	0.56
			Medulla	1787.67	124.32	1790.49	84.40	−0.50	209.60	4.23	0.51
		ROI	Cortex	1521.14	200.02	1522.07	118.23	−1.59	395.99	9.40	0.25
			Medulla	1966.83	225.52	1967.67	230.63	−1.21	602.11	11.05	0.10

▶ **Table 3** (Continuation)

Parameter	Unit	Segmentation		Baseline		Follow-up		Bias (%)	RC	WCV (%)	ICC
				Mean	SD	Mean	SD				
T2 map	ms	MOS	Total kidney	89.12	6.00	97.57	6.00	−1.49	14.73	5.93	0.19
		ROI	Cortex	87.38	7.80	90.23	7.00	−3.85	17.87	7.26	0.31
			Medulla	88.19	7.13	91.64	7.00	−4.50	19.79	7.95	0.04
Volume	mL	MOS	Total kidney	102.07	20.42	100.47	20.06	0.98	18.51	6.56	0.87
			Cortex	41.42	12.28	40.55	7.79	−3.20	21.12	18.78	0.01
		AOS	Total kidney	99.11	20.03	100.01	20.23	−2.09	29.00	10.51	0.74

Discussion

In this study, we evaluated a multiparametric functional non-contrast protocol for renal MRI concerning test-retest repeatability of parameters when acquired with manual segmentation, ROI analysis, and automatic segmentation.

In contrast to preceding studies applying multiparametric renal MRI protocols [17, 41, 42, 43, 44], our study comprises several new aspects concerning evaluation of functional MRI of the kidneys. We applied a broad selection of functional MR parameters inspired by the PARENCHIMA recommendations with differing new features. We implemented a 3 D single-shot PCASL research sequence for improved SNR and reduced motion artifacts in perfusion imaging. Our protocol also included a diffusion-weighted single-shot EPI prototype sequence with reduced field of view (zoomed) for IVIM imaging, where b-values from 0 to 800 s/mm^2 were applied and 2 sets of DWI data acquired with the phase-encoding direction were reversed to enable the geometric distortion correction resulting from EPI acquisition. Different models exist for DWI, the most common being the monoexponential model with the measurement of the apparent diffusion coefficient (ADC), the biexponential model (IVIM,) and diffusion tensor imaging (DTI) [26, 45]. Several studies have shown improved representation of the diffusion-weighted signal in kidneys with IVIM compared to ADC [46, 47, 48]. DTI also provides additional information by measuring the directional dependence (anisotropy) of apparent diffusion in the tissue [49]. In our study, we did not use DTI, since no navigator-triggered acquisition was provided for this sequence by the manufacturer. Alternative acquisition methods would have been measurement under free breathing without triggering, which is accompanied by severe motion artifacts, or the use of a respiratory belt, which proved no reliable sequence triggering in our experience. Moreover, the additional acquisition time would have exceeded the examination time of our protocol for possible application in clinical settings.

Evaluation of our multiparametric functional MRI protocol concerning test-retest repeatability showed that our study results were in the range of preceding studies [17, 41, 42, 43, 44]. As reported in previous studies, repeatability was better for structural measurements such as T1 and T2 mapping and DWI compared to functional measurements including ASL and BOLD [41]. The repeatability of RBF and f results between test and retest measurements was lowest compared to the other evaluated parameters. It is also known that both RBF and f are very sensitive parameters influenced by various physiological changes such as hydration [50]. It is, therefore, unclear if the low repeatability is a limitation of the technique or if there is a true difference in the perfusion of the kidney between the first and the second measurement. As recommended [24], we instructed the volunteers to pay attention to sufficient hydration during the day and avoid fluids and larger meals 2 h before the examination. Examinations were conducted at the same time of day for test and retest measurements to minimize physiological changes due to the circadian rhythm [25]. However, there is no evidence whether these arrangements help to reduce artifacts and improve repeatability. BOLD imaging is known to be sensitive to magnetic susceptibility artifacts, which we also identified especially in the region of the left colic flexure,

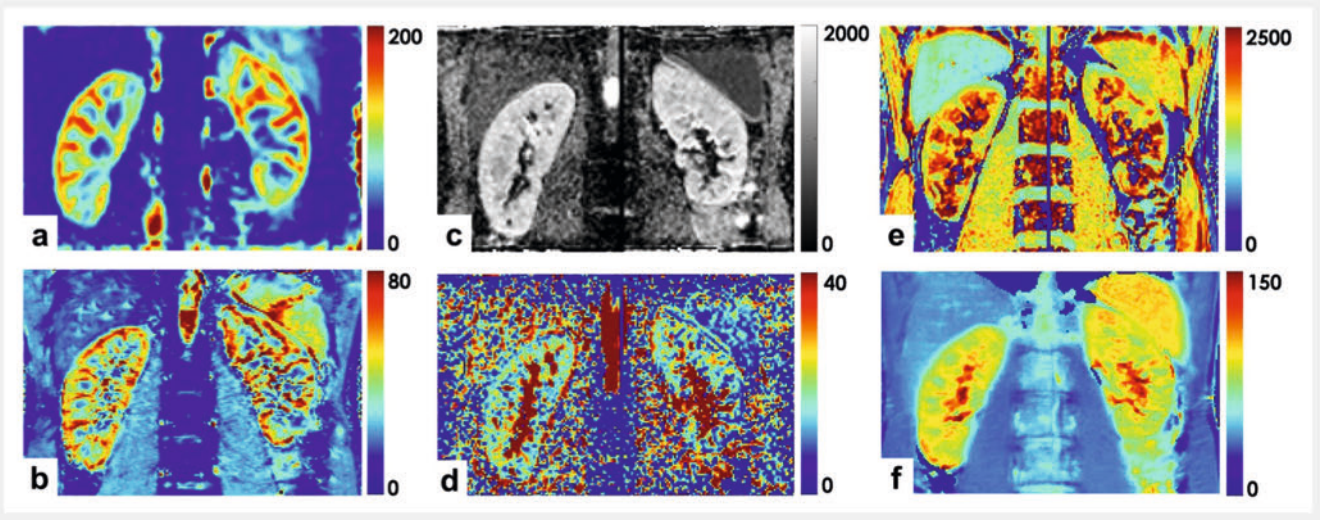

▶ **Fig. 2** Quantitative images of a healthy volunteer examined with a multiparametric functional MRI protocol: **a** renal blood flow (RBF) derived from ASL (ml/min/100 g), **b** T2* map (ms), **c** D map (10^{-6} mm^2/s), **d** perfusion fraction (f, %), **e** T1 VFA (ms), **f** T2 map (ms).

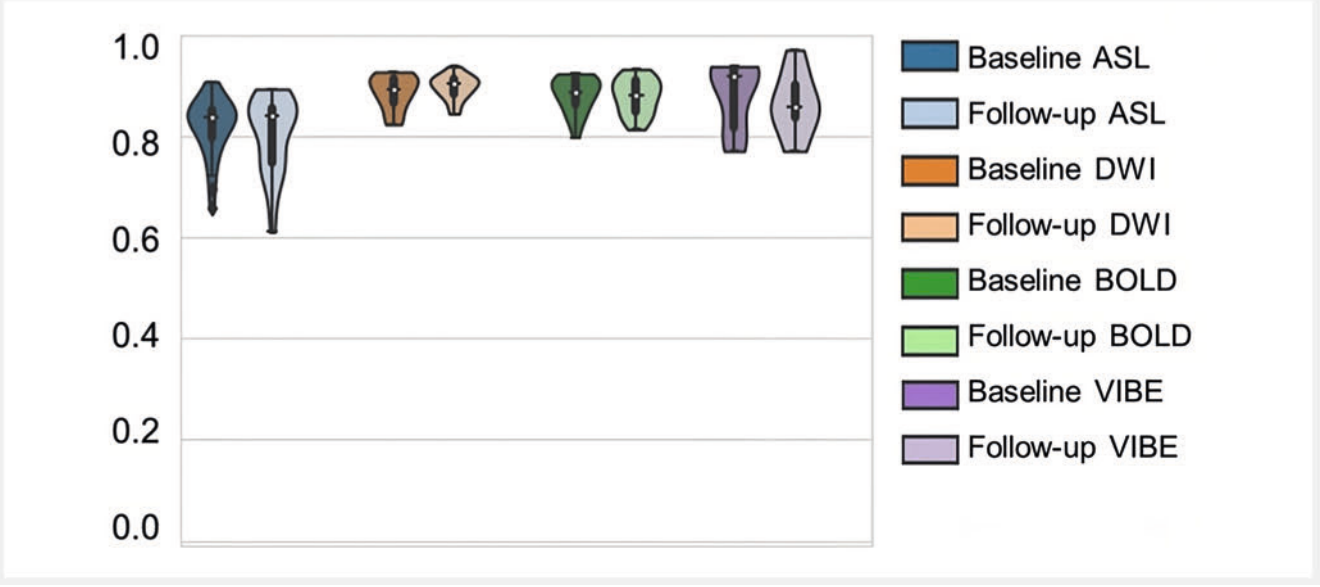

▶ **Fig. 3** Dice scores across different MR parameters: ASL, DWI, BOLD, and VIBE.

probably due to intestinal gas. This might have affected the repeatability of BOLD measurements in the left kidney and resulted in higher overall wCVs compared to results of the right kidney. The awareness of the range of variation of values due to physiological changes is crucial for clinical studies to differentiate between physiological and pathological values. For instance, the median bias between the test and retest measurement of RBF in our study ranged between 1 % and 23 % depending on the image analysis technique. In a study applying a multiparametric MRI protocol for assessing kidney function in patients with acute kidney injury by Buchanan et al., differences between approximately 40 % and 60 % between time points of renal recovery could be measured [51]. Repeatability of MRI parameters might differ depending on the technical details of the applied protocol, which is why test-retest studies for individual study protocols are crucial.

Besides the evaluation of the repeatability of functional renal MRI parameters, our study included a comparison between different image analysis strategies for assessing quantitative MRI results.

Different image analysis strategies posed different challenges. Manual segmentation of renal compartments was not possible for all MR parameters since several parameter maps such as diffusion and T2 maps provided no corticomedullary image contrast. If the corticomedullary contrast is sufficient, the renal cortex can be segmented and medulla masks can be subtracted from the total kidney and cortex masks, except for ASL, where the medullary SNR was too low. Inter-reader agreement between 3 readers per-

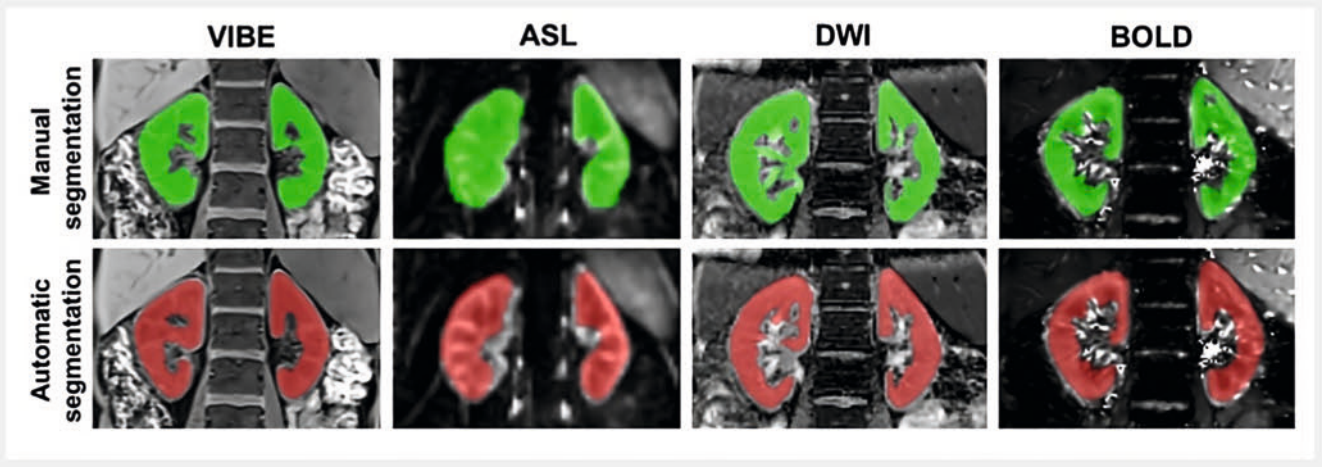

▶ **Fig. 4** Comparison of manual (upper row) and automatic organ segmentation (lower row) of the total kidney across different MR parameters: VIBE, ASL, DWI, and BOLD.

forming manual segmentation on anatomical T1 images was acceptable for the segmentation of the total kidney with Dice scores between 0.79 and 0.86, but poor for segmentation of the cortex with Dice scores between 0.66 and 0.76. Evaluation of manual segmentation masks indicated that readers delineate organ and compartment edges differently, in that they are either more restrictive or extensive in edge definition. The inter-reader difference in edge definition, therefore, mainly affected the inter-reader agreement but not the quantitative analysis of MR parameters.

Automatic segmentation of total kidney volume was performed for ASL, DWI, BOLD, and VIBE. Despite the relatively small amount of training data, the nnUNet framework yielded acceptable segmentation accuracy with Dice scores between 0.86 and 0.91. Segmentation performance for ASL was poorer compared to the other investigated contrast agents. This was likely due to the inherently greater variability in signal intensity in RBF maps and low SNR compared to the other contrast agents. As a limitation, automatic segmentation of the cortex and medulla was not included in the training.

By applying different image analysis strategies in this study, we evaluated the effect of image analysis methods on the repeatability of quantitative MR results. For most of the MRI parameters, our study outcomes showed comparable results concerning repeatability with manual and automatic segmentation of total kidney volume. ROI analysis in the cortex and medulla, however, showed significantly lower repeatability in nearly all MR parameters compared to manual segmentation of the cortex and medulla. One exception was perfusion measurements with ASL, where repeatability results were relatively low for all image analysis strategies. ROI analysis has been a common image analysis method in the past decades, when automatic segmentation was not available yet and fast image analysis for quantitative results was needed. This image analysis strategy seems to be a relatively impartial method for easily assessing quantitative image information. However, it also includes the risk of sampling error. A higher number of ROIs could reduce the risk of sampling errors but would also diminish the advantage of time efficiency compared to laborious manual organ segmentation. Manual segmentation proves to be the most reliable image analysis technique which enables segmentation of all visible macroscopic structures. It is, however, by far the most laborious and also reader-dependent image analysis technique, as was indicated by the low inter-reader agreement and low repeatability of manual cortex segmentation. Therefore, a limitation of this study was also that manual segmentation and ROI analysis of all parameters was performed by only one reader. Automatic segmentation based on the nnUNet framework presented acceptable segmentation accuracy in our study despite the small data set. Still, it is unclear how accurate the results would be for corticomedullary differentiation. Evaluation of different automatic segmentation strategies with various approaches and larger data sets is needed to further promote automatic segmentation for a broader application and thereby also support renal MRI research with faster and more efficient image analysis. Further standardization is needed for both renal MRI protocols and image analysis strategies to enable multicenter studies and examination of different renal pathologies and finally to pave the way to clinical application of multiparametric functional MRI of the kidneys.

Conclusion

Reasonable test-retest repeatability could be achieved with our multiparametric functional MRI protocol including ASL, IVIM, BOLD, T1 and T2 mapping, and volumetry. For further evaluation, typical deviations and uncertainties of measured values have to be compared to disease-related effects. Evaluation of different image analysis strategies concerning repeatability showed overall superior repeatability of manual segmentation to ROI analysis of the cortex and medulla, while automatic segmentation of the total kidney displayed similar repeatability to manual segmentation. Awareness of the repeatability limits of the applied MR parameters and image analysis techniques is crucial for the differentiation between physiological and technical variance and pathologi-

cal results when it comes to diagnostic imaging in patients with kidney disease. These findings encourage the development and improvement of image analysis techniques and support broader application of multiparametric functional MRI for kidney diagnostics and future clinical studies.

Funding Information

Wilhelm Sander-Stiftung (2020.143.1) | http://dx.doi.org/10.13039/100008672

Conflict of Interest

The authors declare that they have no conflict of interest.

Clinical Trial

Registration number (trial ID): DRKS00018966 | German Clinical Trials Register (https://drks-neu.uniklinik-freiburg.de/) | Type of Study: Prospektive single-center study

References

[1] Odudu A, Nery F, Harteveld AA et al. Arterial spin labelling MRI to measure renal perfusion: a systematic review and statement paper. Nephrol Dial Transplant 2018; 33: ii15–ii21. doi:10.1093/ndt/gfy180

[2] Caroli A, Schneider M, Friedli I et al. Diffusion-weighted magnetic resonance imaging to assess diffuse renal pathology: a systematic review and statement paper. Nephrol Dial Transplant 2018; 33: ii29–ii40. doi:10.1093/ndt/gfy163

[3] Pruijm M, Mendichovszky IA, Liss P et al. Renal blood oxygenation level-dependent magnetic resonance imaging to measure renal tissue oxygenation: a statement paper and systematic review. Nephrol Dial Transplant 2018; 33: ii22–ii28. doi:10.1093/ndt/gfy243

[4] Wolf M, de Boer A, Sharma K et al. Magnetic resonance imaging T1- and T2-mapping to assess renal structure and function: a systematic review and statement paper. Nephrology, dialysis, transplantation : official publication of the European Dialysis and Transplant Association – European Renal Association 2018; 33: ii41–ii50

[5] Zhang J, Zhang LJ. Functional MRI as a Tool for Evaluating Interstitial Fibrosis and Prognosis in Kidney Disease. Kidney Diseases 2020; 6: 7–12. doi:10.1159/000504708

[6] Yu YM, Ni QQ, Wang ZJ et al. Multiparametric functional magnetic resonance imaging for evaluating renal allograft injury. Korean journal of radiology 2019; 20: 894. doi:10.3348/kjr.2018.0540

[7] Wang F, Takahashi K, Li H et al. Assessment of unilateral ureter obstruction with multi-parametric MRI. Magnetic Resonance in Medicine 2018; 79: 2216–2227

[8] Schutter R, Lantinga VA, Borra RJH et al. MRI for diagnosis of post-renal transplant complications: current state-of-the-art and future perspectives. Magnetic Resonance Materials in Physics, Biology and Medicine 2020; 33: 49–61

[9] Schley G, Jordan J, Ellmann S et al. Multiparametric magnetic resonance imaging of experimental chronic kidney disease: A quantitative correlation study with histology. PloS one 2018; 13: e0200259

[10] Pruijm M. Can COMBINED Magnetic Resonance Imaging Measure the Progression of Kidney Disease? Clinical journal of the American Society of Nephrology : CJASN 2020; 15: 747–749. doi:10.2215/CJN.04430420

[11] Mao W, Ding X, Ding Y et al. Evaluation of interstitial fibrosis in chronic kidney disease by multiparametric functional MRI and histopathologic analysis. European radiology 2023; 33: 4138–4147. doi:10.1007/s00330-022-09329-7

[12] MacAskill CJ, Erokwu BO, Markley M et al. Multi-parametric MRI of kidney disease progression for autosomal recessive polycystic kidney disease: mouse model and initial patient results. Pediatric research 2021; 89: 157–162. doi:10.1038/s41390-020-0883-9

[13] Li X-M, Yang L, Reng J et al. Non-invasive evaluation of renal structure and function of healthy individuals with multiparametric MRI: Effects of sex and age. Scientific Reports 2019; 9: 10661

[14] Lang ST, Guo J, Bruns A et al. Multiparametric quantitative MRI for the detection of IgA nephropathy using tomoelastography, DWI, and BOLD imaging. Investigative radiology 2019; 54: 669–674. doi:10.1097/RLI.0000000000000585

[15] Gillis K, Rankin A, Allwood-Spiers S et al. P0289 MULTI-PARAMETRIC RENAL MAGNETIC RESONANCE IMAGING IN EARLY KIDNEY TRANSPLANTATION. Nephrol Dial Transplant 2020; 35: gfaa142.P0289

[16] Eckerbom P, Hansell P, Cox E et al. Multiparametric assessment of renal physiology in healthy volunteers using noninvasive magnetic resonance imaging. American Journal of Physiology-Renal Physiology 2019; 316: F693–F702. doi:10.1152/ajprenal.00486.2018

[17] Cox EF, Buchanan CE, Bradley CR et al. Multiparametric Renal Magnetic Resonance Imaging: Validation, Interventions, and Alterations in Chronic Kidney Disease. Frontiers in physiology 2017; 8: 696. doi:10.3389/fphys.2017.00696

[18] Buchanan CE, Mahmoud H, Cox EF et al. Quantitative assessment of renal structural and functional changes in chronic kidney disease using multi-parametric magnetic resonance imaging. Nephrology, dialysis, transplantation : official publication of the European Dialysis and Transplant Association – European Renal Association 2020; 35: 955–964

[19] Boer A de, Harteveld AA, Stemkens B et al. Multiparametric Renal MRI: An Intrasubject Test–Retest Repeatability Study. Journal of magnetic resonance imaging 2021; 53: 859–873. doi:10.1002/jmri.27167

[20] Adams LC, Bressem KK, Scheibl S et al. Multiparametric Assessment of Changes in Renal Tissue after Kidney Transplantation with Quantitative MR Relaxometry and Diffusion-Tensor Imaging at 3 T. Journal of clinical medicine 2020; 9: 1551

[21] Caroli A, Pruijm M, Burnier M et al. Functional magnetic resonance imaging of the kidneys: where do we stand? The perspective of the European COST Action PARENCHIMA. Nephrol Dial Transplant 2018; 33: ii1–ii3. doi:10.1093/ndt/gfy181

[22] Mendichovszky I, Pullens P, Dekkers I et al. Technical recommendations for clinical translation of renal MRI: a consensus project of the Cooperation in Science and Technology Action PARENCHIMA. Magn Reson Mater Phy 2020; 33: 131–140. doi:10.1007/s10334-019-00784-w

[23] Home | Parenchima. 2021. https://renalmri.org/

[24] Bane O, Mendichovszky IA, Milani B et al. Consensus-based technical recommendations for clinical translation of renal BOLD MRI. Magn Reson Mater Phy 2020; 33: 199–215. doi:10.1007/s10334-019-00802-x

[25] Nery F, Buchanan CE, Harteveld AA et al. Consensus-based technical recommendations for clinical translation of renal ASL MRI. Magn Reson Mater Phy 2020; 33: 141–161. doi:10.1007/s10334-019-00800-z

[26] Ljimani A, Caroli A, Laustsen C et al. Consensus-based technical recommendations for clinical translation of renal diffusion-weighted MRI. Magn Reson Mater Phy 2020; 33: 177–195. doi:10.1007/s10334-019-00790-y

[27] Dekkers IA, Boer A de, Sharma K et al. Consensus-based technical recommendations for clinical translation of renal T1 and T2 mapping MRI. Magn Reson Mater Phy 2020; 33: 163–176. doi:10.1007/s10334-019-00797-5

[28] Zollner FG, Kocinski M, Hansen L et al. Kidney Segmentation in Renal Magnetic Resonance Imaging – Current Status and Prospects. IEEE Access 2021; 9: 71577–71605

[29] Günther M, Oshio K, Feinberg DA. Single-shot 3D imaging techniques improve arterial spin labeling perfusion measurements. Magnetic Resonance in Medicine 2005; 54: 491–498. doi:10.1002/mrm.20580

[30] Andersson JLR, Skare S, Ashburner J. How to correct susceptibility distortions in spin-echo echo-planar images: application to diffusion tensor imaging. Neuroimage 2003; 20: 870–888. doi:10.1016/S1053-8119(03)00336-7

[31] Buxton RB, Frank LR, Wong EC et al. A general kinetic model for quantitative perfusion imaging with arterial spin labeling. Magnetic Resonance in Medicine 1998; 40: 383–396

[32] Robson PM, Madhuranthakam AJ, Smith MP et al. Volumetric Arterial Spin-labeled Perfusion Imaging of the Kidneys with a Three-dimensional Fast Spin Echo Acquisition. Academic radiology 2016; 23: 144–154

[33] Smith SM, Jenkinson M, Woolrich MW et al. Advances in functional and structural MR image analysis and implementation as FSL. Neuroimage 2004; 23: S208–19. doi:10.1016/j.neuroimage.2004.07.051

[34] Andersson JLR, Graham MS, Drobnjak I et al. Towards a comprehensive framework for movement and distortion correction of diffusion MR images: Within volume movement. Neuroimage 2017; 152: 450–466

[35] Le Bihan D, Breton E, Lallemand D et al. Separation of diffusion and perfusion in intravoxel incoherent motion MR imaging. Radiology 1988; 168: 497–505. doi:10.1148/radiology.168.2.3393671

[36] Pekar J, Moonen CT, van Zijl PC. On the precision of diffusion/perfusion imaging by gradient sensitization. Magnetic Resonance in Medicine 1992; 23: 122–129. doi:10.1002/mrm.1910230113

[37] Gilliam C, Kustner T, Blu T. 3D motion flow estimation using local all-pass filters. 2016 IEEE International Symposium on Biomedical Imaging: From Nano to Macro:Wednesday, 13 April-Saturday, 16 April 2016, Clarion Congress Hotel in Prague, Czech Republic. Piscataway, NJ: IEEE; 2016: 282–285

[38] Kellner E. Nora – The Medical Imaging Platform. 2022. https://www.nora-imaging.com/#team

[39] Isensee F, Jaeger PF, Kohl SAA et al. nnU-Net: a self-configuring method for deep learning-based biomedical image segmentation. Nature Methods 2021; 18: 203–211. doi:10.1038/s41592-020-01008-z

[40] Chen LC, Papandreou G, Kokkinos I et al. DeepLab: Semantic Image Segmentation with Deep Convolutional Nets, Atrous Convolution, and Fully Connected CRFs. IEEE Trans. Pattern Anal. Mach. Intell 2018; 40: 834–848

[41] Boer A de, Harteveld AA, Stemkens B et al. Multiparametric Renal MRI: An Intrasubject Test-Retest Repeatability Study. Journal of magnetic resonance imaging : JMRI 2021; 53: 859–873. doi:10.1002/jmri.27167

[42] Kline TL, Edwards ME, Garg I et al. Quantitative MRI of kidneys in renal disease. Abdom Radiol 2018; 43: 629–638. doi:10.1007/s00261-017-1236-y

[43] Li LP, Thacker J, Li W et al. Consistency of Multiple Renal Functional MRI Measurements Over 18 Months. Journal of magnetic resonance imaging: JMRI 2018; 48: 514–521. doi:10.1002/jmri.26001

[44] Rankin AJ, Allwood-Spiers S, Lee MMY et al. Comparing the interobserver reproducibility of different regions of interest on multi-parametric renal magnetic resonance imaging in healthy volunteers, patients with heart failure and renal transplant recipients. Magnetic Resonance Materials in Physics, Biology and Medicine 2020; 33: 103–112

[45] Caroli A, Schneider M, Friedli I et al. Diffusion-weighted magnetic resonance imaging to assess diffuse renal pathology: a systematic review and statement paper. Nephrol Dial Transplant 2018; 33: ii29–ii40. doi:10.1093/ndt/gfy163

[46] Blondin D, Lanzman RS, Mathys C et al. Funktionelle MRT der Transplantatnieren: klinische Wertigkeit der Diffusionsbildgebung. Fortschr Röntgenstr 2009; 181: 1162–1167

[47] Ljimani A, Lanzman RS, Müller-Lutz A et al. Non-gaussian diffusion evaluation of the human kidney by Padé exponent model. Journal of magnetic resonance imaging : JMRI 2018; 47: 160–167. doi:10.1002/jmri.25742

[48] Schneider MJ, Dietrich O, Ingrisch M et al. Intravoxel Incoherent Motion Magnetic Resonance Imaging in Partially Nephrectomized Kidneys. Investigative radiology 2016; 51: 323–330. doi:10.1097/RLI.0000000000000244

[49] Notohamiprodjo M, Reiser MF, Sourbron SP. Diffusion and perfusion of the kidney. European journal of radiology 2010; 76: 337–347. doi:10.1016/j.ejrad.2010.05.033

[50] Zöllner FG, Šerifović-Trbalić A, Kabelitz G et al. Image registration in dynamic renal MRI-current status and prospects. Magma (New York, N.Y.) 2020; 33: 33–48

[51] Buchanan C, Mahmoud H, Cox E et al. Multiparametric MRI assessment of renal structure and function in acute kidney injury and renal recovery. Clinical Kidney Journal 2020; 1: 8. doi:10.1093/ckj/sfaa221